Supporting Information

Nuclease Resistant DNA *via* High-Density Packing in Polymeric Micellar Nanoparticle Coronas

Anthony M. Rush, Matthew P. Thompson, Erick T. Tatro[‡], and Nathan C. Gianneschi[*,†]

[†]Department of Chemistry & Biochemistry, University of California, San Diego, 9500 Gilman Drive, La Jolla, CA 92093-0303, United States

[‡]Department of Psychiatry, University of California San Diego, 9500 Gilman Drive, La Jolla, California 92093-0603, United States

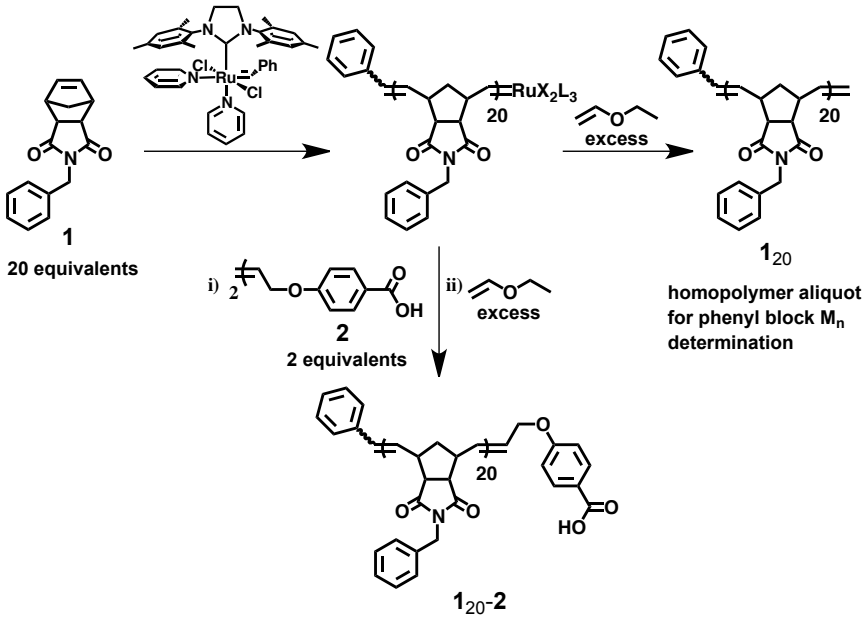

Figure S1. Carboxylic acid-terminated polymer synthesis via ROMP.

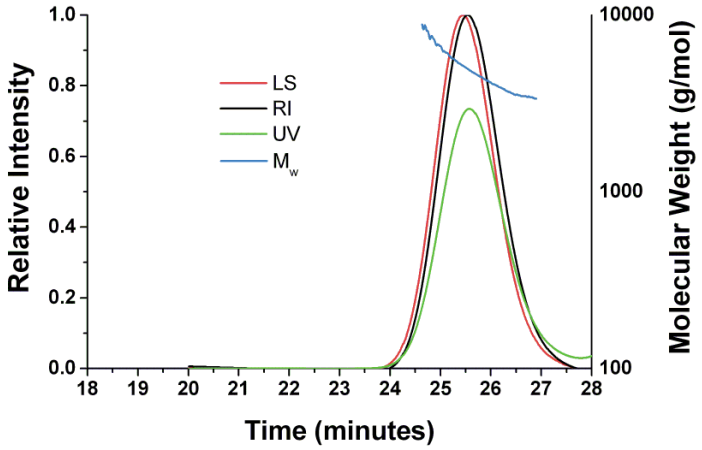

Figure S2. Polymer $\mathbf{1}_{20}$ SEC-MALS chromatogram (LS = light scattering Rayleigh ratio, RI = refractive index difference, UV = UV absorbance at 280 nm, Mw = polymer molecular weight).

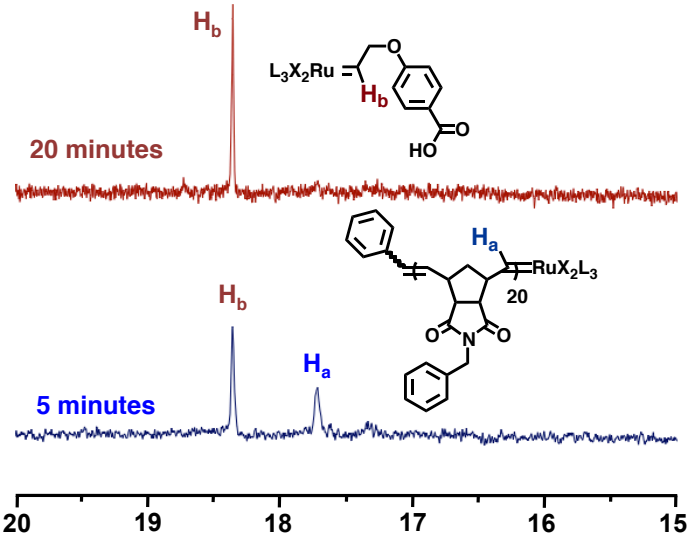

Figure S3. ^{1}H NMR overlay showing complete termination of ROMP polymer with termination agent **2** (x-axis = δ in ppm). The resonance of the alkylidine proton in the polymeric species is at 17.7 ppm. Upon termination with compound **2**, an alkylidine proton resonance corresponding to the metathesis product appears at 18.4 ppm. At 20 minutes, the resonance corresponding to the polymeric species is absent, indicating completion of the polymer termination reaction. At this point ethyl vinyl ether is added to quench the catalyst.

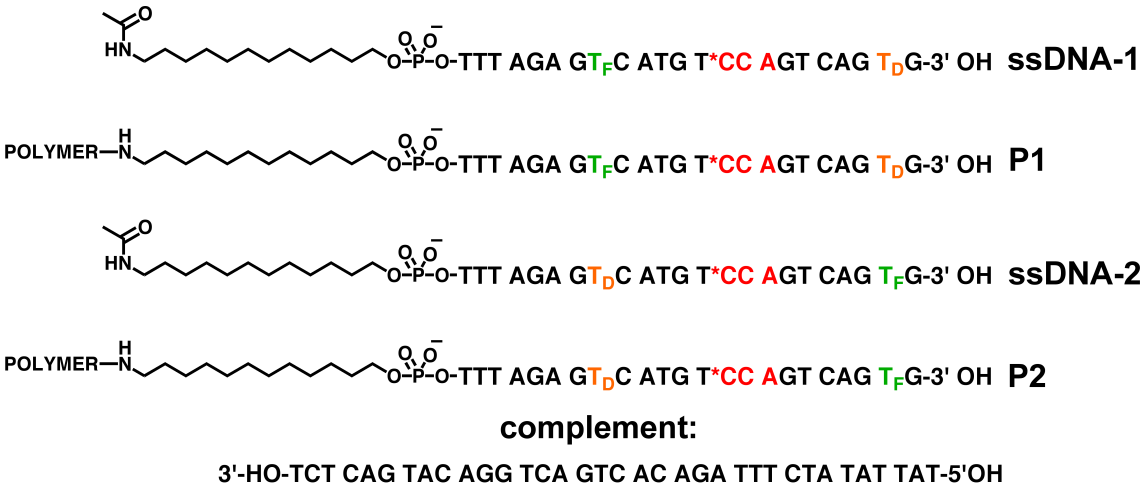

Figure S4. DNA sequences and chemical modifications. The recognition site for Nt.CviPII is indicted in red and the nick site is indicated by an asterisk. T_D and T_F indicate Dabcyl and Fluorescein labeled bases respectively.

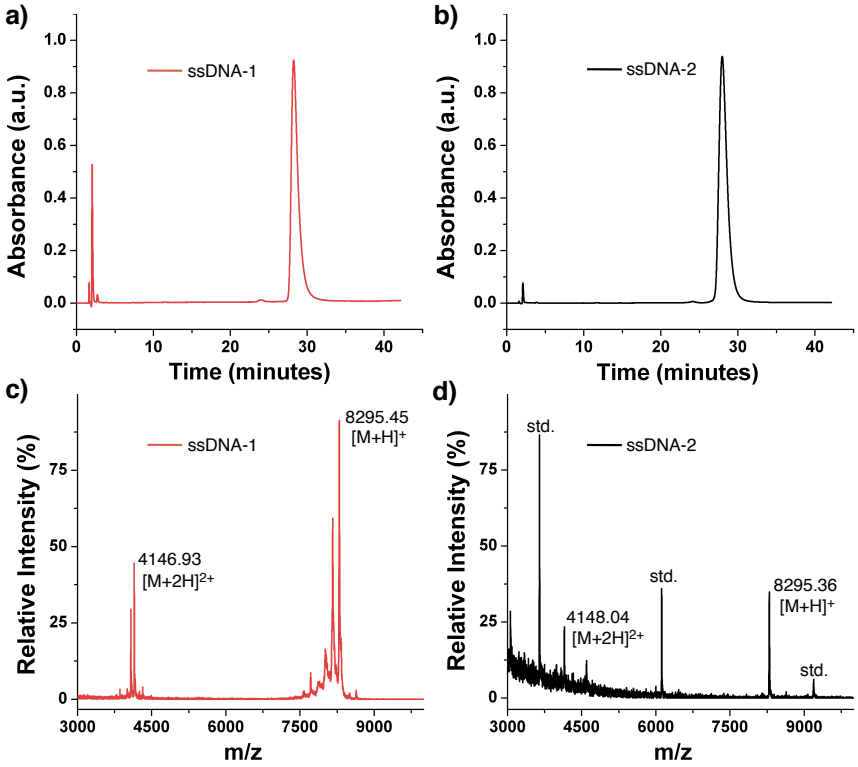

Figure S5. HPLC purification and MALDI-TOF analysis of ssDNA-1 and ssDNA-2**.** a) HPLC chromatogram of purified ssDNA-1 (λ_{abs} = 290nm, gradient: 36-60% B in 50 minutes). b) HPLC chromatogram of purified ssDNA-2 (λ_{abs} = 290nm, gradient: 36-60% B in 50 minutes). c) MALDI-TOF mass spectrum of ssDNA-1, m/z = obs: 8295.45; theo: 8292.07 (calibration was performed externally). d) MALDI-TOF mass spectrum of ssDNA-2, m/z = obs: 8295.36; theo: 8292.07 (calibration was performed internally, left-to-right std. m/z = obs: 3646.21; theo: 3646.4, obs: 6118.48; theo: 6118.0, obs: 9191.64; theo: 9192.0).

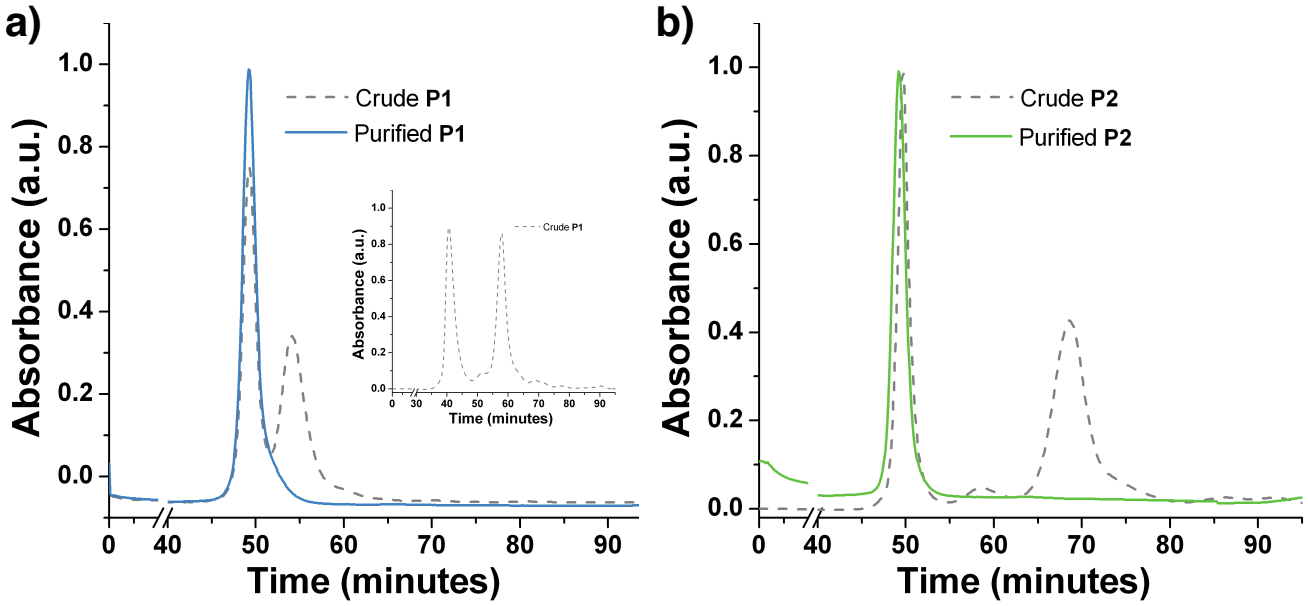

Figure S6. Companion of Figure 1. SEC FPLC purification of DPA nanoparticles **P1** and **P2.**

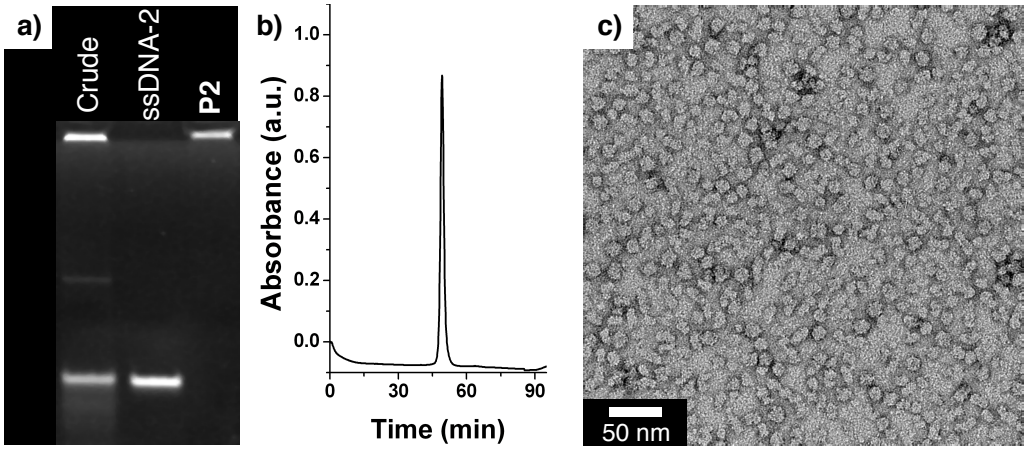

Figure S7. Companion of Figure 1. Characterization of pure **P2** DPA-nanoparticles. a) PAGE analysis. Lane 1: Crude material post-micelle (**P2**) formation showing conjugate (top band) and free ssDNA (lower band). Lane 2: HPLC purified sample of ssDNA-2. Lane 3: Purified **P2**, isolated via size-exclusion chromatography (SEC-FPLC). b) SEC trace of purified **P2** (λ_{abs}=260 nm). c) Transmission electron micrograph of **P2**.

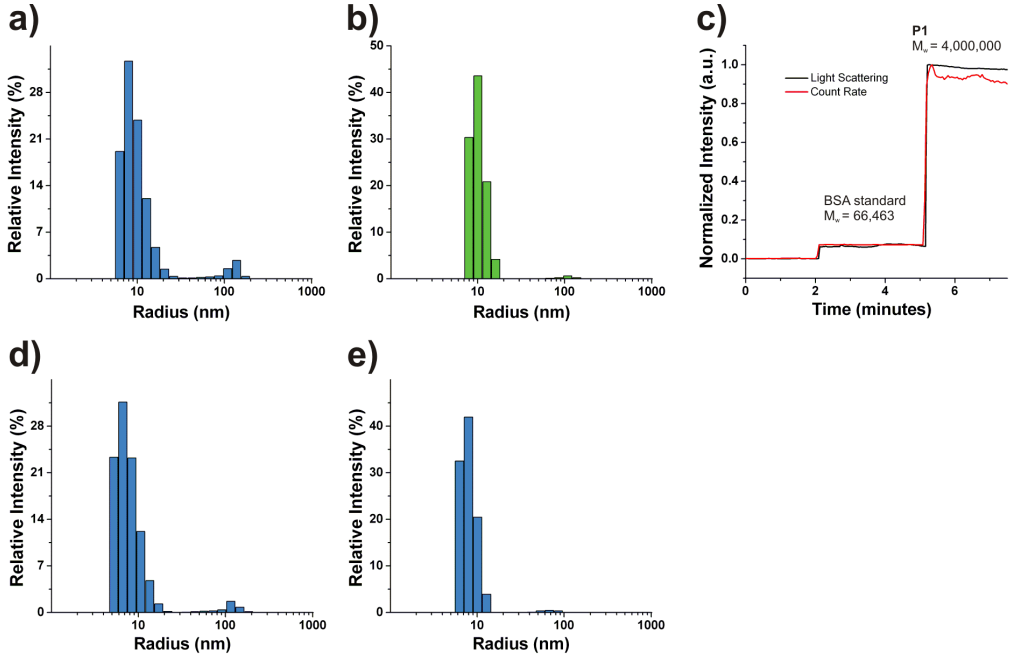

Figure S8. Light scattering data for DPA nanoparticles **P1** and **P2**. a) DLS histogram for **P1** showing aggregates with a hydrodynamic diameter of 20 nm (10 mM Tris pH 8.5, 25 °C, mass weighted intensity signal). b) DLS histogram for **P2** showing aggregates with a hydrodynamic diameter of 20 nm (10 mM Tris pH 8.5, 25 °C, mass weighted intensity signal). c) SLS/DLS analysis of **P1** versus BSA protein standard, M_w = 4,000,000 g/mol, N_{agg} = 295 DPA/nanoparticle (DPA M_w = 5221 g/mol (polymer) + 8295 g/mol (oligo) = 13516 g/mol; 4,000,000/13516 = 295, 295/(4*3.14*(10^2)) = 0.23 DNA/nm^2). d) DLS histogram of **P1** in Exo III reaction buffer at 37 °C showing stability against aggregation. Potassium acetate was added in order to prevent aggregation due to $MgCl_2$ in NE Buffer 1. e) DLS histogram of **P1** in Nt.CviPII reaction buffer at 37 °C showing stability against aggregation.

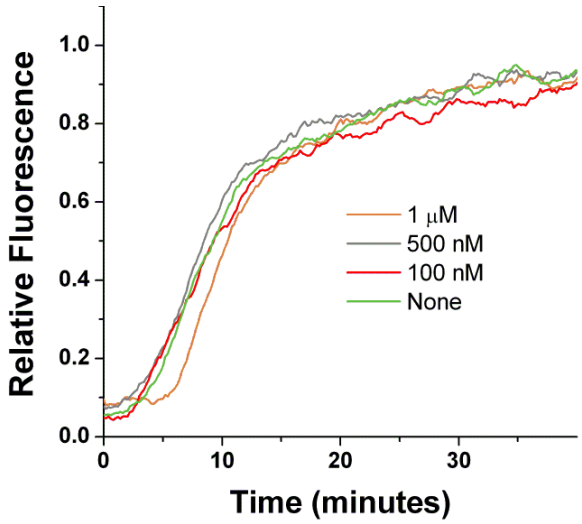

Figure S9. Indiscriminate Exo III activity on ss (green) and ds DNA (red, grey, orange) substrates.

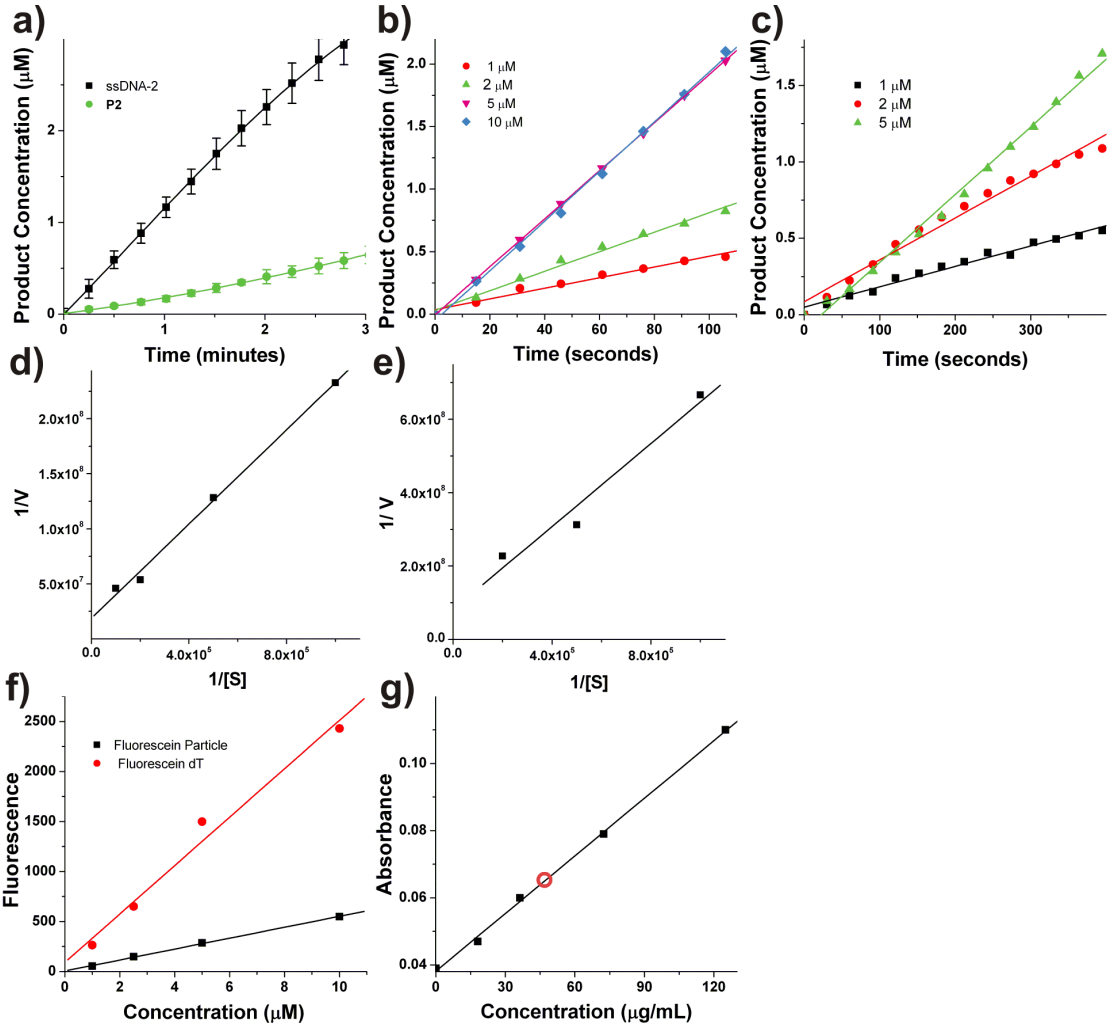

Figure S10. Companion of Table 1. Exo III kinetic analysis against ssDNA-2 and **P2**. a) Exo III activity, shown as fluorescence de-quenching over time for ssDNA-2 and **P2**, plotted as concentration of liberated fluorescein dT. b) Initial rate data for Exo III vs. ssDNA-2 at varying concentrations of ssDNA-2. c) Initial rate data for Exo III vs. **P2** at varying concentrations of **P2**. d) Lineweaver-Burk plot for Exo III activity on ssDNA-2. e) Lineweaver-Burk plot for Exo III activity on **P2**. f) Fluorescein dT fluorescence calibration curve showing a linear increase in fluorescence with increasing concentration of the free phosphoramidite (red). Shown in black is an analogous calibration curve for a DPA-nanoparticle identical to **P1** but not containing a DABCYL quencher moiety. The drastic difference in slopes for the two fluorescent systems is indicative of the unique environment of the fluorescein molecule on the nanoparticle. g) Bradford assay calibration curve (black) constructed using BSA standard and dye reagent (Bio-Rad #500-0002). Exo III sample is plotted in red, indicative of a concentration of 55 μg/mL.

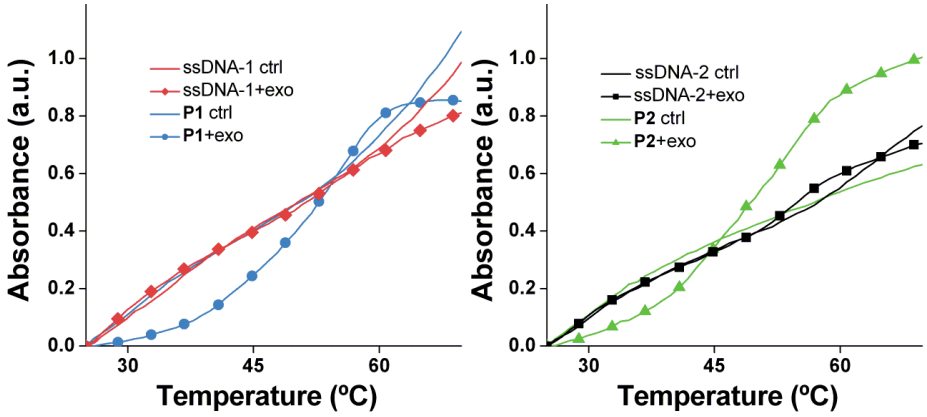

Figure S11. Companion of Figure 3 d,e. DNA melting temperature analysis with and without Exo III treatment. For substrate plus Exo III, the experiment was conducted as described in the text. For substrate control melting curves, the substrate (ssDNA or DPA-nanoparticle) was treated in an identical fashion to those in the experiments except no enzyme or complementary DNA was added before conducting melting temperature analysis. Furthermore, complementary DNA on its own was analyzed in a similar fashion (ie no ssDNA, particle, or enzyme present). The absorbance spectra for this complement on its own was added to that of the control ssDNA or DPA nanoparticle to produce the control spectrum (solid lines without symbols) in the above figures. This comparison highlights the fact that ssDNA, after digestion with Exo III, is unable to form a significant duplex with its complement. Therefore, ssDNA-1 and ssDNA-2 exhibit featureless melting curves identical to the sum of the absorbance curves for both ssDNA strands on their own.

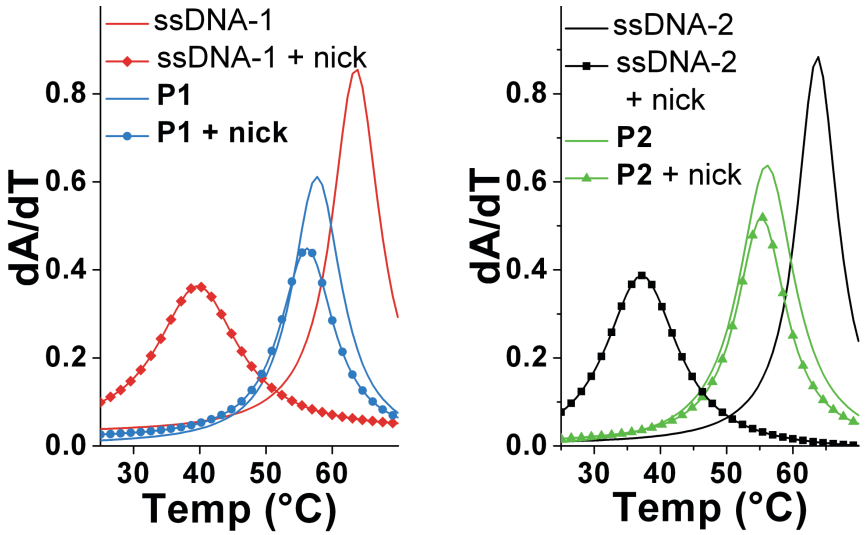

Figure S12. Companion of Figure 2. Derivative plots of thermal denaturation analysis with and without Nt.CviPII treatment for ssDNA-1, **P1** (left) and ssDNA-2, **P2** (right).

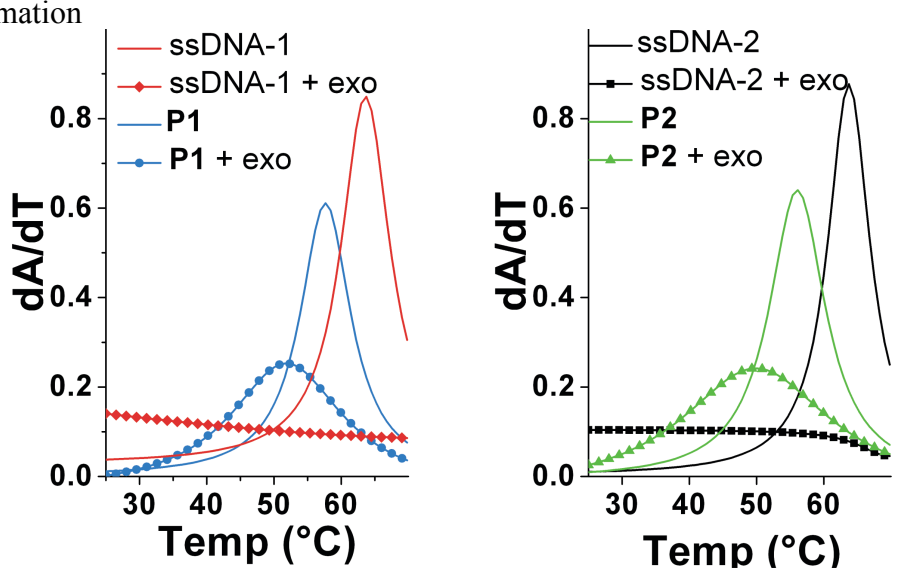

Figure S13. Companion of Figure 3. Derivative plots of thermal denaturation analysis with and without ExoIII treatment for ssDNA-1and **P1** (left), and ssDNA-2 and **P2** (right).

Materials and Methods

All reagents were purchased from commercial sources and used without further purification. $(IMesH_2)(C_5H_5N)_2(Cl)_2Ru{=}CHPh$ was prepared as described by Sanford *et. al.*[1] DNA synthesis was carried out on an ABI 394 DNA/RNA synthesizer utilizing standard phosphoramidite chemistry. DNA synthesis reagents and custom phosphoramidites were purchased from Glen Research Corporation. CPG support columns and standard phosphoramidites were purchased from Azco Biotech Inc. Nucleases Nt.CviPII and Exonuclease III were purchased from New England Biolabs. Phosphodiesterase I from *Crotalus adamanteus* was purchased from USB Corporation as a lyophilized powder. All deuterated solvents were purchased from Cambridge Isotope Laboratories Inc. ^{1}H (400 MHz) and ^{13}C (100 MHz) NMR spectra were recorded on a Varian Mercury Plus spectrometer. Chemical shifts (^{1}H) are reported in δ (ppm) relative to the $CDCl_3$ residual proton peak (7.27 ppm). ^{13}C chemical shifts are reported in δ (ppm) relative to the $CDCl_3$ carbon peak (77.00 ppm). Mass spectra were obtained at the UCSD Chemistry and Biochemistry Molecular Mass Spectrometry Facility. Low-resolution mass spectra were obtained using a Thermo LCQdeca mass spectrometer and high-resolution mass spectra were obtained using an Agilent 6230 Accurate Mass time of flight mass spectrometer. Polymer molecular weight and polydispersity were determined via size-exclusion chromatography (Phenomenex Phenogel 5u 10, 1K-75K, 300 x 7.80 mm in series with a Phenomex Phenogel 5u 10, 10K-1000K, 300 x 7.80 mm (mobile phase: 0.05 M LiBr in DMF)) using a Hitachi-Elite LaChrom L-2130 pump equipped with a DAWN HELEOS multi-angle light scattering (MALS) detector (Wyatt Technology) and a refractive index detector (Hitachi L-2490) normalized to a 30,000 g/mol polystyrene standard. Hydrodynamic diameter

(D_h) of DPA nanoparticles was measured via DLS using a DynaPro NanoStar (Wyatt Technology). DPA nanoparticle molecular weight was determined via batch mode SLS using a DAWN HELEOS MALS detector. Concentrations of oligonucleotides, DPA nanoparticles, and fluorescein phosphoramidite standards were determined using a Thermo Scientific NanoDrop 2000c spectrophotometer. HPLC analysis and purification of oligonucleotides was accomplished utilizing a Phenomenex Clarity 5u Oligo-RP (150 x 4.60 mm) or Clarity 10u Oligo-WAX (150 x 4.60 mm) column and a Hitachi-Elite LaChrom L-2130 pump equipped with a UV-Vis detector (Hitachi-Elite LaChrom L-2420). Oligonucleotide molecular weights were determined by mass spectrometry performed on a Bruker Daltronics Biflex IV MALDI-TOF instrument using a combination of 2', 4', 6'-trihydroxyacetophenone monohydrate (THAP) and 3-hydroxypicolinic acid (3-HPA) as matrices and a three-point calibration standard (Oligonucleotide Calibration Standard #206200, Bruker). Denaturing polyacrylamide gel electrophoresis was performed using a Bio Rad Criterion Mini-PROTEAN Tetra cell and precast TBE-Urea gels. Size-exclusion FPLC was accomplished using a HiPrep 26/60 Sephacryl S-200 High Resolution-packed size-exclusion column (mobile phase: 10 mM Tris, 0.5 mM EDTA pH 8.3) and an Äkta purifier (Pharmacia Biotech) equipped with a P-900 pump and a UV-900 UV-Vis multi-wavelength detector. TEM samples were deposited on carbon/formvar-coated copper grids (Ted Pella Inc.), stained with 1% w/w uranyl acetate, and imaged using a Technai G2 Sphera operating at an accelerating voltage of 200 kV. Fluorescence data were acquired using a Perkin Elmer HTS 7000 Plus Bio Assay Reader (excitation filter: IB14326, B126002, EX-A, emission filter: IB21654, B126103, EM-A). DNA melting temperature analysis was conducted using a Beckman Coulter DU 640 spectrophotometer equipped with a high performance temperature controller. Enzyme kinetics were calculated using Lineweaver-Burk plot analysis with enzyme concentrations determined via a standard Bradford assay.

REFERENCES

1. Sanford, M. S.; Love, J. A.; Grubbs, R. H. A Versatile Precursor for the Synthesis of New Ruthenium Olefin Metathesis Catalysts. *Organometallics* **2001**, *20*, 5314-5318.